Nonlinear optical absorption and temporal response of arsenic- and oxygen-implanted GaAs

M. J. Lederer[a] and B. Luther-Davies
Laser Physics Centre, Research School of Physical Sciences and Engineering, The Australian National University, Canberra, 0200 ACT, Australia

H. H. Tan and C. Jagadish
Electronic Material Engineering, Research School of Physical Sciences and Engineering, The Australian National University, Canberra, 0200 ACT, Australia

M. Haiml, U. Siegner, and U. Keller
Institute of Quantum Electronics, Swiss Federal Institute of Technology, ETH Hönggerberg-HPT, CH-8093 Zürich, Switzerland

(Received 4 September 1998; accepted for publication 8 February 1999)

We have measured the nonlinear optical absorption of arsenic and oxygen implanted epitaxial GaAs for a range of ion doses and annealing temperatures. The response time, τ_A, and a parameter, $M_{\max}$, which characterizes the performance of the structures as modulators, are both reduced by implantation, and correspondingly the nonbleachable losses are increased. We show that similar combinations of (τ_A, $M_{\max}$) can be achieved using either ion species and various combinations of dose and annealing temperatures. Furthermore, the data were all located on a well-defined curve in the (τ_A, $M_{\max}$) plane, provided amorphization, which occurs at high implant doses, was avoided. We deduce that there exists a limit to the modulation if a specific response time is required. © *1999 American Institute of Physics.* [S0003-6951(99)00914-6]

Semiconductor saturable absorbers have become popular for applications in passive mode locking of solid-state lasers[1] and all-optical switching.[2] In both cases it is beneficial to have fast response times ($\tau_A \approx 1$ ps) while retaining as much modulation as possible. There are two main approaches to the generation of a short τ_A in semiconductors. One involves growth at low temperature (LT) using molecular beam epitaxy (MBE);[3] the other is via ion implantation[4,5] of high temperature grown material. LT-MBE growth has been used extensively for the fabrication of semiconductor saturable absorber mirrors (SESAMs) for passive mode locking,[1] and more recently ion-implanted SESAM devices were also demonstrated.[6] In this letter we present a comprehensive study of the nonlinear optical absorption modulation and response times of arsenic As- and oxygen O-implanted GaAs saturable absorbers annealed under different conditions. We show that similar combinations of modulation and response time can be realized using either ion species for various combinations of dose and annealing conditions, demonstrating that a rather general relation exists between modulation and response time in annealed ion implanted GaAs.

Our test structures were grown using metal organic chemical vapor deposition (MOCVD) and consisted of a Bragg reflector followed by 500 nm of GaAs. The Bragg mirror was centered at $\lambda = 830$ nm and had a typical reflectivity of greater than 99% over a range of 70 nm. After growth the samples were implanted with 700 keV As ions or 250 keV O ions with doses ranging from 8×10^{10} to $1 \times 10^{16}\,\mathrm{cm}^{-2}$ and annealed at 500, 600, or 700 °C for 20 min under arsine overpressure, or remained unannealed. For both ion species the displacement distribution lay solely inside the 500 nm GaAs layer. After implantation and annealing we applied an 830 nm antireflection (AR) coating to the samples to minimize Fabry–Perot effects. All optical measurements were done in reflection.

We performed two types of measurements using 830 nm, 80 MHz, 100 fs pulse trains. First, we measured the fluence dependent reflectivity $R(F_p) = P_{\mathrm{out}}/P_{\mathrm{in}}$ using single beam excitation. Note that, due to the AR coating, changes in $R(F_p)$ were dominated by absorption bleaching in the GaAs layer causing the reflectivity to increase. Since the underlying Bragg mirror is nonabsorbing for wavelengths above 750 nm it does not contribute to the nonlinear response but merely acts as a 100% reflector. Typical traces of reflectivity versus pulse fluence are shown in Fig. 1 for unimplanted as well as $8 \times 10^{13}\,\mathrm{cm}^{-2}$ O-implanted, 500 °C/20 min annealed samples. The experimental data were fitted numerically using a model for a traveling wave, two level saturable absorber.[7] The fit is excellent for the most interesting fluence range whereas the disagreement found for fluences higher than $0.5\,\mathrm{mJ\,cm}^{-2}$ is mainly attributed to two photon and free carrier absorptions [(TPA) and (FCA)], which were not included in the model. The latter effects also account for the incomplete bleaching achieved in unimplanted GaAs. The numerical fits identified both the maximum modulation depth, ΔR and the nonbleachable losses, ΔR_{ns}, consistently between samples, neglecting TPA and FCA. Figure 1 clearly shows that the modulation of the ion-implanted sample is smaller compared with the unimplanted case, and that ΔR_{ns} has increased. In general we have found that ΔR_{ns} increases and ΔR decreases for higher doses or lower annealing temperatures. For instance, in Fig. 1 the O-implanted sample has $\Delta R = 0.39$ and $\Delta R_{\mathrm{ns}} = 0.26$ which compares with the values for the unimplanted sample where $\Delta R_{\mathrm{GaAs}} = 0.59$ and $\Delta R_{\mathrm{ns,\,GaAs}} = 0.1$. We attribute these changes to deep levels,

[a]Electronic mail: MJL111@rsphysse.anu.edu.au

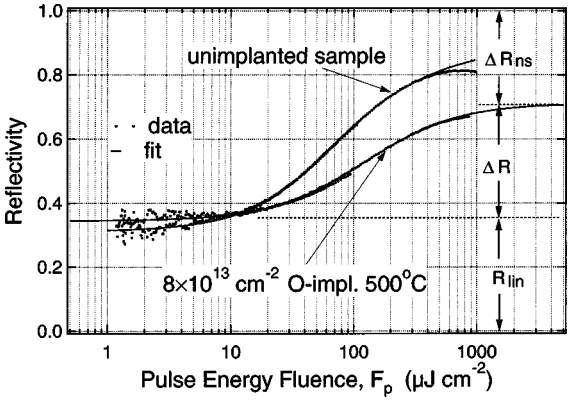

FIG. 1. Reflectivity as a function of the pulse energy fluence, F_p, for the unimplanted as well as $8\times10^{13}\,\mathrm{cm}^{-2}$ O-implanted 500 °C/20 min annealed samples.

created by the implantation, which give rise to additional transitions to states high in the bands. We expect that these transitions are difficult to bleach due to the large density of states high in the bands. The deep level transitions also contribute to the linear absorption resulting in a smaller linear reflectivity R_{lin}. However, our data show that any change in R_{lin} was smaller than the uncertainty of ±0.05, arising from slight differences in the AR coatings of different samples. This explains the slightly higher R_{lin} of the O-implanted sample compared to the unimplanted case. Since $R_{\mathrm{lin}}+\Delta R+\Delta R_{\mathrm{ns}}\approx1$ any increase in ΔR_{ns} primarily corresponded to a reduction of ΔR.

In the second, pump-probe measurement we determined the time resolved differential reflectivity for different pump fluences using pump-probe delays as long as 300 ps. As an example, Fig. 2 shows the normalized differential reflectivity, *dR*, for O-implanted samples for different doses and annealing conditions compared with the unimplanted case. The pump-excited carrier density in the probed volume was approximately $2.5\times10^{18}\,\mathrm{cm}^{-3}$ at a pump fluence of 28 $\mu\mathrm{J\,cm}^{-2}$. As in the first measurement, the dominating mechanism causing the reflectivity change is absorption bleaching in the GaAs layer. Contributions to *dR* originating from changes in the real part of the complex refractive index of GaAs are negligible for our structures. This was confirmed

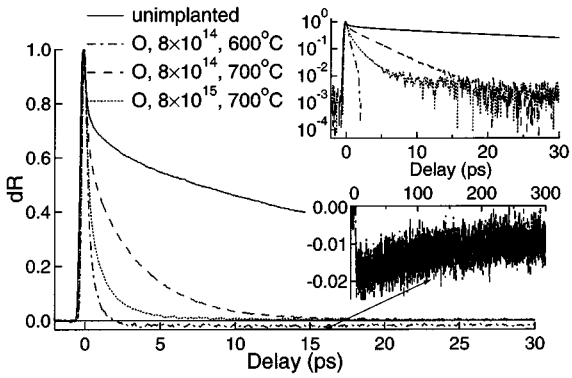

FIG. 2. Normalized differential reflectivity *dR* of different O-implanted samples compared with the unimplanted sample. The insets show log and linear plots of signal evolution and PIA, respectively. The carrier density in the probed volume is approximately $2.5\times10^{18}\,\mathrm{cm}^{-3}$, $F_p=28\,\mu\mathrm{J\,cm}^{-2}$. Ion doses are in cm^{-2}.

through modeling assuming typical index changes <0.1. In all samples we observed a multiexponential response corresponding to carrier thermalization and cooling within the first several 100 fs, and trapping and recombination via deep-level traps introduced by ion implantation. As is apparent from the sample data in Fig. 2, for increasing implantation dose or decreasing annealing temperature we obtained faster capturing-related signal decay indicating that the density of deep-level traps is higher for these conditions, as would be expected. Furthermore, the fastest signals decay with effectively a single exponential with time constants <200 fs and are dominated by carrier capturing, masking even the cooling process. Signals dominated by fast capturing evolve to negative differential reflectivity, i.e., photoinduced absorption (PIA), leveling off at a *dR* value, usually a few percent or less, below zero. This is then followed by very slow (several 100 ps) evolution to $dR=0$ (see inset in Fig. 2). This has been similarly observed in LT-GaAs,[8] and attributed to slow recombination of captured carriers which provide additional transitions from midgap to high levels in the bands, after bleaching from band filling has ceased due to fast and complete capturing. In contrast to the case of LT-GaAs,[8] we did not observe any slow residual bleaching attributable to completely filled traps even at excitation densities $>1\times10^{19}\,\mathrm{cm}^{-3}$. Further studies are needed to clarify the recombination dynamics. The nature and density of deep level traps in ion implanted GaAs is a research topic of current interest. Recently, it has been shown that, similar to LT-GaAs, ionized As antisites ($\mathrm{As}_{\mathrm{Ga}}^{+}$) are present in implanted and annealed GaAs.[9] These deep level traps may also play a role in our samples.

Using the results of the modulation and pump-probe measurements, we have characterized the different samples by plotting their modulation behavior normalized to that of unimplanted GaAs, using the parameter $M_{\max}=(\Delta R/1-R_{\mathrm{lin}})(1-R_{\mathrm{lin,\,GaAs}}/\Delta R_{\mathrm{GaAs}})$, against an effective recovery time τ_A. For consistency with previous work, τ_A was defined as the delay after which *dR* had decayed to $1/e$ times its peak value. Note that annealing was very effective in removing implant-induced changes in R_{lin}, and hence for our annealed samples $M_{\max}\approx\Delta R/\Delta R_{\mathrm{GaAs}}$. However, $M_{\max}$ was introduced for generality since a reduction in R_{lin} (even if $\Delta R_{\max}$ remained unaffected after implantation), should be reflected by a poorer assessment of modulator performance, and this would be masked if the potential effect of R_{lin} were omitted. Samples implanted with different ions, doses, and annealed under different conditions are, therefore, represented as points in the (τ_A, $M_{\max}$) plane. This is shown in Fig. 3 for the complete set of annealed samples. The unannealed samples are not shown because, although extremely fast, their *M* value was very low and varied due to *in situ* annealing under high excitation, making them less suitable for applications.

There is a clear tendency for the data to fall on a well-defined curve relating the achievable modulation to the speed of recovery. Unimplanted GaAs is located on the right hand side of this graph while increasing the implant dose, for a particular annealing condition, progressively moves the data to the left (shorter τ_A and smaller $M_{\max}$). On the other hand, increased annealing temperatures, at a particular implanta-

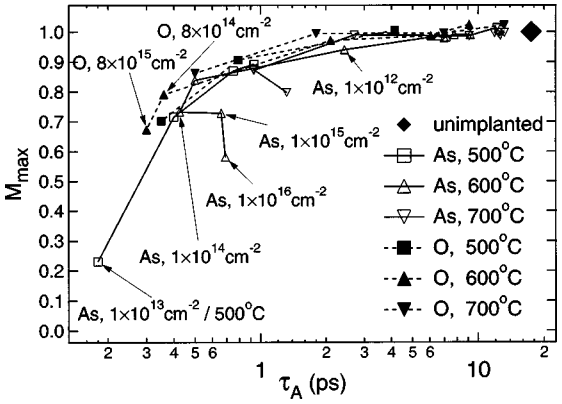

FIG. 3. (τ_{eff}, $M_{\max}$) plane with all annealed samples, each represented by a single point.

tion dose, moves the points back to the right (towards longer τ_A and larger $M_{\max}$). Generally more than an order of magnitude higher dose is required using an O-implant compared with As to achieve the same combination of response time and modulation depth. Figure 3 underlines the fact that a specific (τ_A, $M_{\max}$) combination can be achieved by using a range of different combinations of ion species, doses, and annealing conditions. This suggests that the types of defects in annealed As- and O-implanted GaAs are quite similar and the projected curve defines a rather general relationship between τ_A and $M_{\max}$.

There are, however, outlying cases. First, for As doses above $1\times10^{12}\,\text{cm}^{-2}$, annealed at 500 °C/20 min, $M_{\max}$ drops rapidly while τ_A becomes pulse width limited, increasing the uncertainty on the location of the point As, $1\times10^{13}\,\text{cm}^{-2}$, 500 °C/20 min. Second, As doses above $1\times10^{14}\,\text{cm}^{-2}$ actually reverse the general trend, such that while $M_{\max}$ decreases τ_A increases. This is apparent in the lines for As, 600 °C/20 min and 700 °C/20 min, the latter indicating also the irreversibility of the change even at higher annealing temperatures. The departure most likely indicates a change in nature or composition of the defects created by the implantation process. Earlier time resolved differential reflectivity measurements on unannealed H^+-implanted GaAs[4] revealed a so-called ''lifetime saturation'' which was attributed to the formation of an amorphized layer in the implanted material. In order to investigate this on the microscopic level, we performed Rutherford backscattering spectroscopy-channeling (RBS-C) measurements on the As-implanted samples for doses ranging from 1×10^{13} to $1\times10^{16}\,\text{cm}^{-2}$ before and after annealing at 600 °C/20 min. The RBS-C data reveals that for a dose of $1\times10^{14}\,\text{cm}^{-2}$ a buried amorphous layer was formed in the unannealed sample, which recrystallized upon annealing giving a dechanneling yield only a fraction higher than that of the unimplanted sample. For higher doses the amorphous layer extends both towards the surface and Bragg mirror, recrystallization is very poor after annealing, and RBS-C signals typical of those of extended defects are observed. For nonlinear optical modulator applications implantation doses which generate amorphous layers are clearly undesirable, even if recrystallization is possible, since the onset of a departure from the projected $M_{\max}$ vs τ_A curve can already be observed under these conditions. Note that for O implants higher doses are needed for amorphization since O is lighter than As. This suggests that, with O implantation, shorter τ_A can be obtained since higher doses can be used without amorphization. For instance, the $8\times10^{14}\,\text{cm}^{-2}$ O-implanted, 600 °C/20 min annealed sample achieves a $\tau_A < 400$ fs preserving 80% of the modulation $M_{\max}$ of unimplanted GaAs. It is possible that lighter ions would allow one to produce even shorter τ_A by avoiding amorphization and thereby also preserving the highest possible modulation. A different method of avoiding amorphization would be to implant at elevated temperatures. Figure 3 clearly motivates further study to explore these concepts. Finally, we note that specific devices where the thicknesses of the GaAs absorber is different from that used here will require a change in implant energy which in turn will lead to amorphization occurring at a different dose. Therefore, a generally valid recipe for achieving a specific recovery time through ion implantation for an arbitrary device geometry cannot be given.

In summary, we have studied nonlinear absorption modulation and the recovery time of a large set of As- and O-ion implanted GaAs samples. We showed that both τ_A and $M_{\max}$ decrease through ion implantation with the decrease in $M_{\max}$ being due to increasing nonbleachable losses. It was found that, for doses below amorphization, the data from all annealed samples lie on a well-defined curve in the (τ_A, $M_{\max}$) plane suggesting that the residual defects after annealing are of similar nature and that the curve defines the achievable (τ_A, $M_{\max}$) performance of ion implanted GaAs. Oxygen, being the lighter ion, can be implanted at higher doses than As without amorphization, creating more point defects and shorter τ_A while preserving highest possible modulation. For the $8\times10^{14}\,\text{cm}^{-2}$ O-implanted, 600 °C/20 min annealed sample we measured a $\tau_A < 400$ fs at 80% of the modulation of unimplanted GaAs. Overall, we have shown that ion implantation is a useful and extremely versatile process for making ultrafast absorption modulation devices.

M. J. Lederer acknowledges the support of Electro Optic Systems Pty, Ltd. and the Australian Government for the award of an APA Industry scholarship. H. H. Tan acknowledges the fellowship awarded by the Australian Research Council. The work at ETH Zürich was supported by the Swiss National Science Foundation.

[1] U. Keller, K. Weingarten, I. Kärtner, D. Kopf, B. Braun, I. Jung, R. Fluck, C. Hönninger, N. Matuschek, and J. Aus der Au, IEEE J. Sel. Top. Quantum Electron. **2**, 435 (1996).
[2] R. Takahashi, Y. Kawamura, and H. Iwamura, Appl. Phys. Lett. **68**, 123 (1996).
[3] E. S. Harmon, M. R. Melloch, J. M. Woodall, D. D. Nolte, N. Otsuka, and C. L. Chang, Appl. Phys. Lett. **63**, 2248 (1993).
[4] M. Lambsdorff, J. Kuhl, J. Rosenzweig, A. Axmann, and Jo. Schneider, Appl. Phys. Lett. **58**, 1881 (1991).
[5] A. Krotkus, S. Marcinkevicius, J. Jasinski, M. Kaminska, H. H. Tan, and C. Jagadish, Appl. Phys. Lett. **66**, 3304 (1995).
[6] M. J. Lederer, B. Luther-Davies, H. H. Tan, and C. Jagadish, Appl. Phys. Lett. **70**, 3428 (1997).
[7] L. R. Brovelli, U. Keller, and T. H. Chiu, J. Opt. Soc. Am. B **12**, 311 (1995).
[8] U. Siegner, R. Fluck, G. Zhang, and U. Keller, Appl. Phys. Lett. **69**, 2566 (1996).
[9] H. Fujioka, J. Krueger, A. Prasad, X. Liu, and E. R. Weber, J. Appl. Phys. **78**, 1470 (1995).